BEST AVAILABLE IMAGES

Defective images within this document are accurate representations of the original documents submitted by the applicant.

Defects in the images may include (but are not limited to):

- BLACK BORDERS
- TEXT CUT OFF AT TOP, BOTTOM OR SIDES
- FADED TEXT
- ILLEGIBLE TEXT
- SKEWED/SLANTED IMAGES
- COLORED PHOTOS
- BLACK OR VERY BLACK AND WHITE DARK PHOTOS
- GRAY SCALE DOCUMENTS

IMAGES ARE BEST AVAILABLE COPY.

As rescanning documents *will not* correct images, please do not report the images to the Problem Image Mailbox.

Indian Journal of Chemistry
Vol. 26B, June 1987, pp. 550-555

Antiparasitic Agents: Part VI—Synthesis of 7-Chloro-4-(4-substituted-phenylamino)- & 7-Chloro-4-(4-substituted-piperazin-1-yl)quinolines as Potential Antiparasitic Agents†

VIJAI K AGRAWAL & SATYAVAN SHARMA*
Medicinal Chemistry Division, Central Drug Research Institute, Lucknow 226001

Received 2 June 1986; revised and accepted 21 November 1986

The synthesis of a series of 7-chloro-4-(4-hydroxy-3-substituted-phenylamino)quinolines (9-13, 31-40, 58) and 7-chloro-4-(4-substituted-piperazin-1-yl)quinolines (41-51, 53-59) has been carried out. These compounds have been tested for their antimalarial, antifilarial and antimicrobial activities but none of them shows any noteworthy activity.

The discovery of the human antimalarials[1] chloroquine (1), amodiaquine (2), amopyroquine (3) and cycloquine (4) and the demonstration of filaricidal activity[2,3] by 2 and its various structural analogs like 5, have established the versatility of 4-aminoquinolines in building better drugs for parasite chemotherapy. In a further exploration of the biological profile of 4-aminoquinoline derivatives in malaria and filariasis, a series of 7-chloro-4-(4-hydroxy-3-substituted-phenylamino)quinolines (9-13, 31-40, 58) and 7-chloro-4-(4-substituted-piperazin-1-yl)quinolines (41-51, 53-55) have now been synthesized and evaluated for their antimalarial, antifilarial and antimicrobial activities.

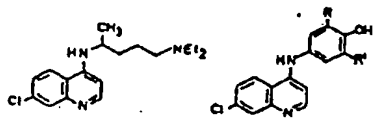

1

2 R=H, R¹=CH₂NEt₂
3 R=H, R¹=CH₃N
4 R=R¹=CH₂NEt₂
5a R=H, R¹=CH₂N⟨⟩N-CH₃
5b R=H, R¹=CH₂N⟨⟩NCONEt₂

Chemistry

Condensation of 4,7-dichloroquinoline (6) with 5-aminosalicylic acid (7) and 4-hydroxy-3-nitroaniline (8) yielded the 7-chloro-4-(4-hydroxy-3-substituted-phenylamino)quinolines 9 and 10 respectively. Attempts to convert 9 into the corresponding amide 31 by reaction of thionyl chloride and pyrrolidine was unsuccessful. In an alternative method, 5-nitrosalicylic acid (14) was treated with thionyl chloride and the resulting acid chloride allowed to react with different amines *in situ* to form the corresponding 5-nitrosalicylamides (15-22). Hydrogenation of 15-22 in the presence of Raney nickel gave the required 5-aminosalicylamides (23-30) which were condensed with 6 to afford 31-38 (Scheme 1).

The synthesis of 7-chloro-4-(4-substituted-phenoxy-phenylamino)quinolines (11-13) was achieved by treating 6 with the corresponding 4-aminodiphenyl ethers while 7-chloro-4-(4-hydroxy-3-aminophenylamino)quinoline (39) was obtained by reduction of 10 with Raney nickel and hydrogen. Treatment of the latter with 1,3-dicarbethoxy-S-methylisothiourea gave 7-chloro-4-[3-(N,N'-dicarbethoxyguanidino)-4-hydroxyphenylamino]quinoline (40) (Scheme 1).

The synthesis of 7-chloro-4-(4-substituted-piperazin-1-yl)quinolines (42-51) was carried out as outlined in Scheme 2. Reaction of 7-chloro-4-piperazin-1-ylquinoline (41)[4], obtained by condensation of piperazine with 6, with different electrophiles yielded 42-45 of which 7-chloro-4-(4-chloroacetylpiperazin-1-yl)quinoline (45) was treated with N,N-diethylcarbamoylpiperazine to afford 7-chloro-4-{4-[α-(4-diethylcarbamoylpiperazin-1-yl)acetyl]piperazin-1-yl}quinoline (46). However, 47-49 were obtained by direct condensation of 41 with desired chloroacetamides. Reaction of 41 with 1,3-dicarbalkoxy-S-methylisothioureas also gave 7-chloro-4-[4-(N,N'-dicarbalkoxyhamidino)piperazin-1-yl]quinolines (50, 51).

Mannich reaction of 4-acetamidophenol (52) with formaldehyde and 41 afforded 7-chloro-4-[4-(5-acetamido-2-hydroxybenzyl)piperazin-1-yl]quinoline (53) which was hydrolysed with dil. HCl to get the corresponding deacetylated product 54. When 54 was allowed to react with 6, 1-(7-chloroquinolin-4-yl)-4-[5-(7-chloroquinolin-4-ylamino)-2-hydroxybenzyl]-piperazine (55) was obtained (Scheme 3).

†CDRI Communication No. 3624

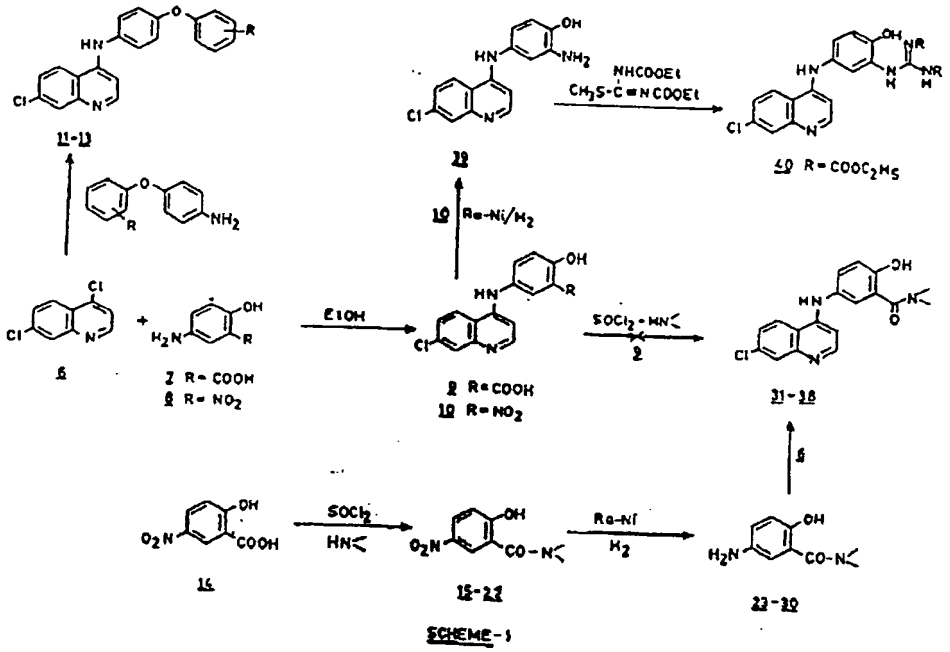

SCHEME-1

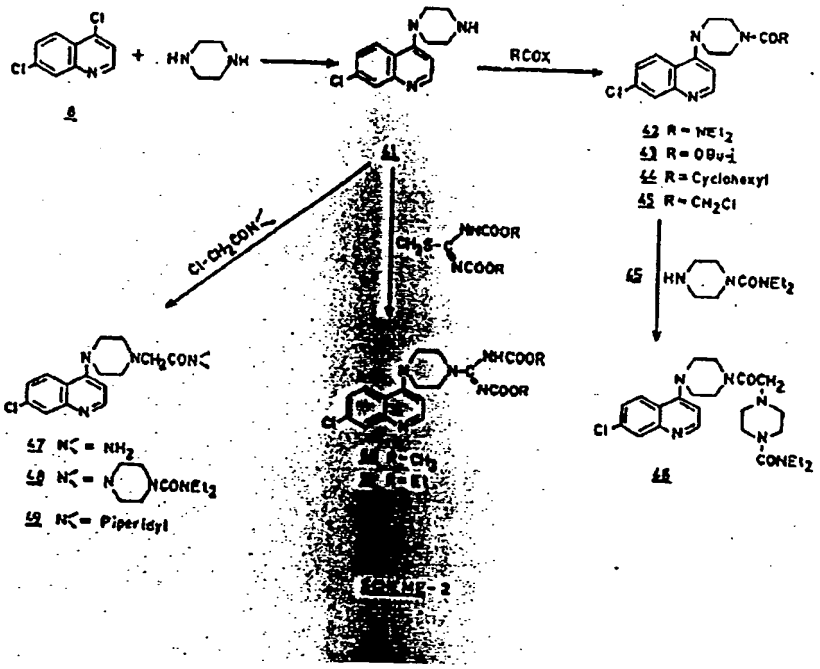

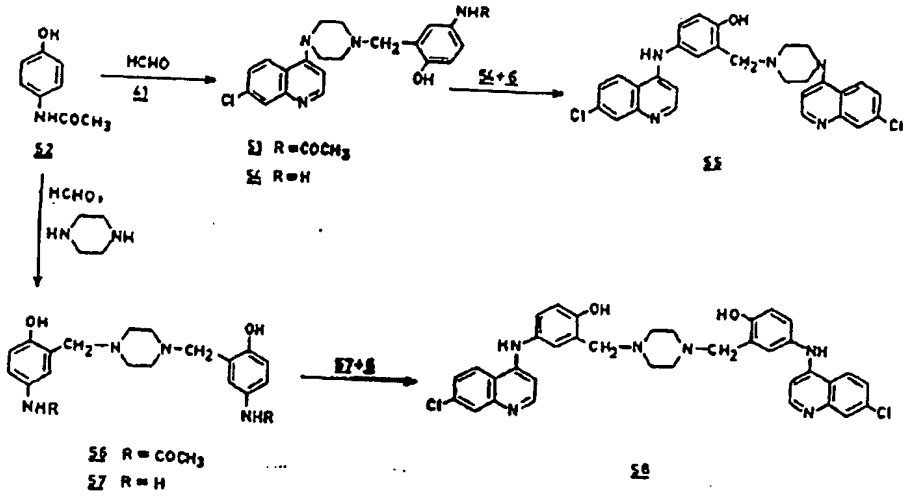

SCHEME - 3

Mannich reaction of 52 with piperazine and formaldehyde led to the formation of 1,4-di(5-acetamido-2-hydroxybenzyl)piperazine (56) which was smoothly hydrolysed in the presence of dil. HCl to yield 57. Condensation of the latter with 4,7-dichloroquinoline (6) afforded 1,4-di[5-(7-chloroquinolin-4-ylamino)-2-hydroxybenzyl]piperazine (58) (Scheme 3).

Biological Activity

Most of the compounds were evaluated for their antimalarial activity against *Plasmodium berghei* in mice and *Plasmodium knowlesi* in monkeys[5]. The screening for antifilarial activity was carried out against *Litomosoides carinii* in cotton rats[6].

The compounds were initially given intraperitoneally to mice infected with *P. berghei* at a dose of 10 mg/kg × 5 days when none of the compounds caused any reduction in blood parasitaemia. Monkeys infected with *P. knowlesi* also received an oral dose of 10 mg/kg for 5 days but none of the compounds showed any noteworthy activity. The compounds were also inactive against *L. carinii* in cotton rats when given intraperitoneally at a dose of 30 mg/kg for 5 days.

In the *in vitro* antimicrobial screening[7] carried out against the bacteria *Staphylococcus aureus* (gram positive, resistant to 2500 units of penicillin/ml), *Salmonella typhi* (gram negative), *Escherichia coli*, *Agrobacterium tumefacience*, *Streptococcus* [illegible] and *Klebsiella pneumonia*, and the fungi *C.* [illegible] *albicans*, *Trichophyton mentagrophytes*, *Cryptococcus neoformans*, *Microsporum canis* and *Aspergillus fumigatus*, none of the compounds inhibited the growth of the microbes upto the minimum inhibitory concentration of 100 μg/ml.

This study clearly indicates the high specificity of 4-aminoquinoline antimalarials against the *Plasmodium* parasites which is evident by the fact that although all the 7-chloro-4-substituted-quinolines carried the biologically accepted pharmacophores, the piperazines and 4-amino-2-substituted-phenols, they did not exhibit antiparastic activity. A similar situation also holds true in the amodiaquine analogs for filaricidal activity.

Experimental Procedure

Melting points were taken in sulphuric acid-bath and are uncorrected. IR spectra were recorded on a Perkin-Elmer 157 infracord spectrometer (ν_{max} in cm^{-1}) and PMR spectra on Perkin-Elmer R 32 and Varian EM-360 instruments using TMS as internal reference (chemical shifts in δ, ppm). Purity of all the compounds was checked by TLC on silica gel G plates and the spots were located by $KMnO_4$ or Dragendorff spray. All the compounds were analysed for C, H and N and the results were within ± 0.4% of the theoretical values.

7-Chloro-4-(3-carboxyl-4-hydroxyphenylamino)quinoline (9)

A solution of 4,7-dichloroquinoline (6; 3.96 g, 0.02 mol) and 5-aminosalicylic acid (7; 3.06 g, 0.02 mol) in ethanol (50 ml) was refluxed for 6 hr. The reaction mixture was cooled and the separated solid filtered, treated with aq. ammonia, filtered and the resulting

solid crystallised from ethanol, yield 3.3 g (52%), m.p. >250°, IR(KBr): 1640 (CO), 3400 (OH) (Found: C, 61.2; H, 3.3; N, 8.7. $C_{16}H_{11}ClN_2O_3$ requires C, 61.1; H, 3.5; N, 8.9%).

Using the above experimental procedure, compounds 10-13 (Table 1) were prepared by the reaction of 6 with corresponding amines.

1-(2-Hydroxy-5-nitrobenzoyl)pyrrolidine (15)

A mixture of 5-nitrosalicylic acid (14; 1.83 g, 0.01 mol) and thionyl chloride (1.1 ml, 0.015 mol) in dry benzene was refluxed for 2 hr, solvent removed and the residue dissolved in dry benzene. To this solution were added pyrrolidine (0.71 g, 0.01 mol) and triethylamine (1.4 ml, 0.01 mol) and the reaction mixture was refluxed for 4 hr, solvent removed *in vacuo* and the residue treated with sodium bicarbonate solution. The separated solid was filtered and crystallised from ethanol, yield 1.2 g (51%), m.p. 210°, IR(KBr): 1620 (CO), 2800 (CH_2), 3400 (OH); PMR($CDCl_3$+DMSO-d_6): 1.7-2.1 [*m*, 4H, $N(CH_2CH_2)_2$], 3.3-3.75 [*m*, 4H, $N(CH_2)_2$], 6.8 (*d*, 1H, Ar–*H*, *o* to OH, J=9 Hz), 7.85-8.2 (*m*, 2H, Ar–*H*, *o* to NO_2) (Found: C, 55.8; H, 5.2; N, 11.6. $C_{11}H_{12}N_2O_4$ requires C, 55.9; H, 5.1; N, 11.9%).

Similarly, compounds 16-22 (Table 1) were prepared by the reaction of 5-nitrosalicylic acid and the corresponding amines.

1-(5-Amino-2-hydroxybenzoyl)pyrrolidine (23)

A suspension of 15 (1.18 g, 0.005 mol) and Raney nickel (~200 mg) in ethanol (30 ml) was shaken with hydrogen in a Paar hydrogenator at 3 kg/cm² pressure for 4 hr. The catalyst was filtered and the filtrate concentrated to get a solid which was used in the next step without purification.

Using the above procedure, compounds 16-22 were reduced to obtain the compounds 24-30 (Table 1) respectively.

7-Chloro-4-(4-hydroxy-3-pyrrolidinoylphenylamino)quinoline (31)

A solution of 6 (0.99 g, 0.005 mol) and 23 (1.03 g, 0.005 mol) in ethanol (25 ml) was refluxed for 6 hr. The reaction mixture was cooled and the separated solid filtered, washed with aq. ammonia, dried and crystallised from ethanol, yield 1.1 g (60%), m.p. 250°; IR(KBr): 1620 (CO), 2900 (CH_2), 3400 (OH); PMR(TFA): 1.6-2.0 [*m*, 4H, $N(CH_2CH_2)_2$], 3.3-3.7 [*m*, 4H, $N(CH_2)_2$], 6.4-8.75 (*m*, 8H, Ar–*H*) (Found: C, 65.1; H, 4.7; N, 11.3. $C_{20}H_{18}ClN_3O_2$ requires C, 65.3; H, 4.9; N, 11.4%).

Similarly, condensation of 6 with 23-30 afforded the compounds 32-38 respectively (Table 1).

7-Chloro-4-(3-amino-4-hydroxyphenylamino)quinoline (39)

It was prepared by the reduction of 7-chloro-4-(4-hydroxy-3-nitrophenyl)aminoquinoline (10; 1.55 g, 0.005 mol) with Raney nickel (~200 mg) as described for the compound 28 and used *in situ* in the next step.

7-Chloro-4-[3-(N,N'-dicarbethoxyguanidino)-4-hydroxyphenylamino]quinoline (40)

A solution of 39 (1.43 g, 0.005 mol) and 1,3-dicarbethoxy-S-methylisothiourea (1.17 g, 0.005 mol) in methanol (50 ml) in the presence of a catalytic amount of PTSA (5 mg) was refluxed for 6 hr. The solid that separated on cooling, was filtered, washed with methanol (2 × 5 ml) and crystallised from ethanol, yield 0.7 g (30%), m.p. 225°; IR(KBr): 1660 (C=N), 1730 (CO); PMR(TFA): 0.9-1.4 (*m*, 6H, 2 × CH_3), 4.0-4.45 (*m*, 4H, 2 × CH_2), 6.5-8.9 (*m*, 8H, Ar–*H*) (Found: C, 55.8; H, 4.5; N, 15.0. $C_{22}H_{22}ClN_5O_5$ requires C, 56.0; H, 4.7; N, 14.9%).

7-Chloro-4-(4-diethylcarbamoylpiperazin-1-yl)quinoline (42)

A solution of diethylcarbamoyl chloride (0.68 g, 0.005 mol) in dry benzene (10 ml) was added dropwise to a cooled and stirred solution of 7-chloro-4-piperazin-1-ylquinoline (41, 1.24 g, 0.005 mol) and triethylamine (0.7 ml, 0.005 mol) in dry benzene (20 ml). The reaction mixture was further stirred at room temperature for 5 hr. The benzene solution was washed with aq. sodium bicarbonate solution, dried (Na_2SO_4), solvent removed and the residue purified by column chromatography over a silica gel column using ethyl acetate as eluant to obtain the product as an oil, yield 1.3 g (73%); IR(neat): 1640 (CO), 2800-3000 (CH_2); PMR($CDCl_3$): 1.6 (*t*, 6H, 2 × CH_3), 2.8-3.5 (*m*, 12H, 6 × CH_2), 6.6-8.6 (*m*, 5H, Ar–*H*) (Found: C, 62.1; H, 6.5; N, 16.4. $C_{18}H_{23}ClN_4O$ requires C, 62.3; H, 6.6; N, 16.1%).

Similarly compounds 43-45 (Table 1) were prepared by the reaction of 41 with the corresponding acid chlorides or alkyl chloroformates.

7-Chloro-4-{4-[α-diethylcarbamoylpiperazin-1-yl)acetyl]piperazin-1-yl}-quinoline (46)

A suspension of 7-chloro-4-(4-chloroacetylpiperazin-1-yl)quinoline (45, 1.62 g, 0.005 mol), 1-diethylcarbamoylpiperazine (0.95 g, 0.005 mol) and sodium carbonate (1 g) in ethanol (50 ml) was refluxed for 8 hr. The reaction mixture was concentrated, water added to the residue and aq. phase extracted with dichloromethane (3 × 50 ml). The combined extracts were dried (Na_2SO_4), concentrated and purified over a silica gel column using ethyl acetate as eluant to get the product as an oil, yield 1.6 g (70%). PMR($CDCl_3$): 1.05

Table I—Physical Data of the Compounds 9-58 Synthesised

Compd	R	N<	Mol. formula	m.p. °C	Yield (%)
9	COOH	—	$C_{16}H_{11}ClN_2O_3$	>250	52
10	NO_2	—	$C_{15}H_{10}ClN_3O_3$	250	65
11	2-OCH_3	—	$C_{23}H_{17}ClN_2O_2$	220	78
12	3-CH_3	—	$C_{23}H_{17}ClN_2O$	196	74
13	4-CH_3	—	$C_{23}H_{17}ClN_2O$	182	80
15	—	Pyrrolidin-1-yl	$C_{11}H_{13}N_3O_4$	210	51
16	—	4-Hydroxy-4-phenyl piperidin-1-yl	$C_{19}H_{19}N_3O_5$	196	60
17	—	4-Diethylcarbamoyl-piperazin-1-yl	$C_{16}H_{22}N_4O_5$	145	55
18	—	4-Methylpiperadin-1-yl	$C_{13}H_{15}N_3O_4$	192	62
19	—	NHEt	$C_9H_{10}N_2O_4$	158	52
20	—	Piperadin-1-yl	$C_{12}H_{13}N_3O_4$	240[a]	60
21	—	$N(Et)_2$	$C_{11}H_{14}N_2O_4$	166[b]	50
22	—	4-Methylpiperazin-1-yl	$C_{12}H_{15}N_3O_4$	138[a]	55
23	—	Pyrrolidin-1-yl	$C_{11}H_{14}N_2O_3$	—[c]	—[c]
24	—	4-Hydroxy-4-phenyl-piperidin-1-yl	$C_{19}H_{20}N_2O_3$	—	—
25	—	4-Diethylcarbamoyl-piperazin-1-yl	$C_{16}H_{24}N_4O_3$	—	—
26	—	4-Methylpiperadin-1-yl	$C_{13}H_{16}N_2O_3$	—	—
27	—	NHEt	$C_9H_{12}N_2O_3$	—	—
28	—	Piperadin-1-yl	$C_{12}H_{14}N_2O_3$	—	—
29	—	$N(Et)_2$	$C_{11}H_{14}N_2O_3$	—	—
30	—	4-Methylpiperazin-1-yl	$C_{13}H_{17}N_3O_3$	—	—
31	—	Pyrrolidin-1-yl	$C_{20}H_{18}ClN_3O_2$	250	60
32	—	4-Hydroxy-4-phenyl-piperadin-1-yl	$C_{27}H_{24}ClN_3O_3$	248	65
33	—	4-Diethylcarbamoyl-piperazin-1-yl	$C_{16}H_{23}ClN_4O$	234	60
34	—	4-Methylpiperadin-1-yl	$C_{22}H_{21}ClN_3O_2$	>250	76
35	—	NHEt	$C_{18}H_{16}ClN_3O_2$	152	54
36	—	Piperadin-1-yl	$C_{21}H_{20}ClN_3O_2$	>250	68
37	—	$N(Et)_2$	$C_{20}H_{20}ClN_3O_2$	>250	50
38	—	4-Methylpiperazin-1-yl	$C_{21}H_{21}ClN_4O_2$	250	55
42	$N(Et)_2$	—	$C_{16}H_{23}ClN_4O$	Oil	73
43	OBu-*t*	—	$C_{19}H_{23}ClN_2O_2$	Oil	70
44	Cyclohexyl	—	$C_{20}H_{24}ClN_3O$	140	62
45	CH_2Cl	—	$C_{14}H_{13}Cl_2N_3O$	Oil	75
47	—	NH_2	$C_{12}H_{17}ClN_4O$	162	60
48	—	4-Diethylcarbamoyl-1-yl	$C_{24}H_{33}ClN_4O_2$	Oil	55
49	—	Piperadin-1-yl	$C_{20}H_{23}ClN_4O$	125	64
50	CH_3	—	$C_{16}H_{20}ClN_4O_4$	80	80
51	Et	—	$C_{20}H_{24}ClN_4O_4$	Oil	75
53	$COCH_3$	—	$C_{23}H_{23}ClN_4O_3$	150	37
54	H	—	$C_{20}H_{21}ClN_4O$	[d]	[d]
55	—	—	$C_{29}H_{25}Cl_3N_3O$	130	45
56	$COCH_3$	—	$C_{32}H_{28}N_4O_4$	260	68
57	H	—	$C_{16}H_{24}N_4O_3$	300	79
58	—	—	$C_{36}H_{32}Cl_2N_4O_2$	286	69

[a]Lit[8], m.p. 245-46°.
[b]Lit[9], m.p. 170-71°.
[c]See ref. 10.
[d]Denotes that the products were used *in situ*. The purity of the compounds was checked by TLC and the yield was taken as quantitative.

(*t*, 6H, 2 × CH_3), 2.42 [*t*, 4H, $CH_2N(CH_2)_2$], 2.5-3.6 (*m*, 18H, 9 × CH_2), 6.6-8.7 (*m*, 5H, Ar—*H*) (Found: C, 60.8; H, 6.9; N, 17.6. $C_{24}H_{33}ClN_6O_2$ requires C, 61.0; H, 7.0; N, 17.8%).

7-Chloro-4-(4-carbamoylmethylpiperazin-1-yl)quinoline (47)

A suspension of 41 (1.24 g, 0.005 mol), α-chloroacetamide (0.47 g, 0.005 mol) and sodium

carbonate (1 g) in ethanol (50 ml) was refluxed for 8 hr, concentrated, the residue taken up in water and aq. phase extracted with dichloromethane (3 × 50 ml). The combined extracts were dried (Na_2SO_4), concentrated and the residue was purified on a silica gel column using ethyl acetate as eluant to get the product as a solid, yield 0.9 g (60%), m.p. 162°, IR(KBr): 1680 (CO), 2800 (CH_2), 3300 (NH_2); PMR($CDCl_3$): 2.85 [*t*, 4H, $CH_2N(CH_2)_2$], 3.05-3.4 [*m*, 6H, $COCH_2$ and $N(CH_2)_2$], 6.7-8.75 (*m*, 7H, Ar–*H* and NH_2) (Found: C, 59.4; H, 5.7; N, 18.2. $C_{15}H_{17}ClN_4O$ requires C, 59.1; H, 5.6; N, 18.4%).

Similarly compounds 48 and 49 (Table 1) were prepared by the condensation of 41 with the corresponding chloroacetyl compounds.

7-Chloro-4-[4-(N,N'-dicarbomethoxyamidino)-piperazin-1-yl]quinoline (50)

A solution of 41 (1.24 g, 0.005 mol) and 1,3-dicarbomethoxy-S-methylisothiourea (1.03 g, 0.005 mol) in ethanol (25 ml) was refluxed for 4 hr, concentrated, triturated with ether and the resulting solid crystallised from ethanol, yield 1.6 g (80%), m.p. 80°, IR(KBr): 1750 (CO), 2800-3000 (CH_2); PMR($CDCl_3$): 3.0-4.0 (*m*, 14H, 2 × CH_3 and 4 × CH_2), 6.7-8.8 (*m*, 5H, Ar–*H*) (Found: C, 53.6; H, 4.8; N, 17.4. $C_{18}H_{20}ClN_5O_4$ requires C, 53.3; H, 4.9; N, 17.3%).

Similarly, 7-chloro-4-[4-(N,N'-dicarbethoxy-amidino)piperazin-1-yl]quinoline (51; Table 1) was prepared by the condensation of 41 with 1,3-dicarbeth xy-S-methylisothiourea.

7-Chloro-4-[4-(5-acetamido-2-hydroxybenzyl)-piperazin-1-yl]quinoline (53)

A solution of 4-acetylaminophenol (52; 1.51 g, 0.01 mol), 41 (2.47 g, 0.01 mol) and 30% aq. formaldehyde (1 ml, 0.01 mol) in ethanol (50 ml) was refluxed for 6 hr, concentrated *in vacuo* and the residual solid crystallised from ethanol, yield 1.5 g (37%), m.p. 150°, IR(KBr): 1680 (CO), 2800-3100 (CH_2), 3500 (OH); PMR(TFA): 2.2 (*s*, 3H, CH_3), 3.3-4.6 (*m*, 10H, 5 × CH_2), 6.8-8.5 (*m*, 8H, Ar–*H*), 9.5 (*s*, 1H, NH) (Found: C, 64.1; H, 5.8; N, 13.5. $C_{22}H_{23}ClN_4O_3$ requires C, 64.3; H, 5.6; N, 13.6%).

Using the above procedure 1,4-di-(5-acetamido-2-hydroxybenzyl)piperazine (56; Table 1) was prepared by the reaction of 52 (2 mol) with anhyd. piperazine (1 mol) and 30% aq. formaldehyde (2 mol).

7-Chloro-4-[4-(5-amino-2-hydroxybenzyl)-piperazin-1-yl]quinoline (54)

A solution of 53 (2.05 g, 0.005 mol) in dil. HCl (30 ml) was refluxed for 3 hr, cooled, basified with aq. ammonia and extracted with ethyl acetate (3 × 50 ml). The combined extracts were dried (Na_2SO_4), concentrated and the residual product was used as such in the next reaction.

Similarly, 1,4-di-(5-amino-2-hydroxybenzyl)-piperazine tetrahydrochloride (57; Table 1) was obtained by the hydrolysis of 56 with HCl.

1-(7-Chloroquinolin-4-yl)-4-[5-(7-chloro-quinolin-4-ylamino)-2-hydroxybenzyl]-piperazine (55)

A solution of 54 (1.84 g, 0.005 mol) and 4,7-dichloroquinoline (6, 0.99 g, 0.005 mol) in ethanol (50 ml) was refluxed for 4 hr, cooled, and the separated solid filtered and treated with aq. ethanol, yield 1.2 g (45%), m.p. 130°, PMR($CDCl_3$): 2.85 [*bs*, 4H, $CH_2N(CH_2)_2$], 3.3 [*bs*, 4H, $N(CH_2)_2$], 3.85 (*s*, 2H, $ArCH_2$), 6.5-8.8 (*m*, 15H, Ar–*H*, OH and NH) (Found: C, 65.9; H, 4.9; N, 13.1. $C_{29}H_{23}Cl_2N_5O$ requires C, 65.7; H, 4.7; N, 13.2%).

Similarly, 1,4-di-[5-(7-chloroquinolin-4-ylamino)-2-hydroxy-benzyl]piperazine (58; Table 1) was prepared by the condensation of 57 (1 mol) with 4,7-dichloroquinoline (6; 2 mol).

Acknowledgement

The authors thank Dr Nitya Anand, for his continued interest and encouragement in the work. They are also grateful to Drs A B Sen, G P Dutta, O P Srivastava and their associates for providing the biological screening results. One of them (V K A) is thankful to ICMR, New Delhi for providing a senior research fellowship.

References

1 Bruce-Chwatt Ed, *Chemotherapy of malaria*, II Ed, (World Health Organisation, Geneva) 1981.
2 Elslager E F, Perricone S C & Tendick F H, *J medni Chem*, 12 (1969) 965.
3 Go M, Ngian T & Wan A S C, *J medni Chem*, 24 (1981) 1471.
4 Singh T, Stein R G, Hoops J F, Biel J H, Hoya W K & Cruz D R, *J medni Chem*, 14 (1971) 283.
5 Peter W, *Exp Parasit*, 17 (1965) 80.
6 Hawking F & Sewell P, *Brit J Pharmacol*, 3 (1948) 285.
7 Dhar M L, Dhar M M, Dhawan B N, Mehrotra B N & Ray C, *Indian J exptl Biol*, 6 (1968) 232.
8 Taborsky R G & Starkey R I, *J pharm Sci*, 52 (1963) 542.
9 Temple Jr C, Rose J D & Montgomery J A, *J medni Chem*, 17 (1974) 972.
10 Sauter F, Stanetty P, Kummerer W & Baradar M, *Arch Pharm*, 311 (1978) 273.

Eur J Med Chem (1995) 30, 395–402

Molecular modeling and quantitative structure–activity studies of anti-HIV-1 2-heteroarylquinoline-4-amines

DB Kireev[1†], JR Chrétien[1*], OA Raevsky[2]

[1]*Laboratoire de Chimiométrie, Université d'Orléans, BP 6759, 45067 Orleans, Cedex 2, France;*
[2]*Institute of Physiologically Active Compounds of Russian Academy of Sciences, 142432, Chernogolovka, Moscow Region, Russia*

(Received 29 June 1994; accepted 5 January 1995)

Summary — Three-dimensional quantitative structure–activity relationships (QSAR), based upon comparative molecular field analysis (CoMFA) and multiple linear regression (MLR) with geometric and quantum chemical descriptors, have been established for a novel class of non-nucleoside HIV-1 inhibitors. The training set consisted of 30 aryl (or heteroaryl) quinoline-4-amines. For the CoMFA model a 'leave-one-out' procedure yielded a cross-validated test $r^2 = 0.602$ consistent with the uncertainty of biological data. The MLR model was obtained using two newly derived descriptors with a conventional correlation coefficient $r = 0.916$. These descriptors were calculated using the results of molecular modeling and a quantum chemical AM1 study. One of the descriptors represents the shape contribution of the amino substituent and the other represents the electrostatic contribution of the aryl or heteroaryl substituent. Together with the MLR model and our previous quantum chemical study, the CoMFA plots provide reasonable guidelines to delineate a pharmacophore for this series of anti-HIV agents.

HIV-1 inhibitor / quantitative structure–activity relationship / molecular modeling / molecular electrostatic potential / quantum chemistry / AM1

Introduction

Nucleoside analogs currently remain the primary agents in the chemotherapy of AIDS. However, their clinical usefulness is counterbalanced by their toxic side effects. Moreover, it was established that at least two or more stages of chemical transformations are necessary for these compounds in the course of their action, *eg*, phosphorylation and incorporation into DNA, and some of these transformations are provided by enzyme catalysis [1]. The above properties make nucleosides difficult for structure–activity analysis and the systematic design of molecules with high selectivity to HIV.

I

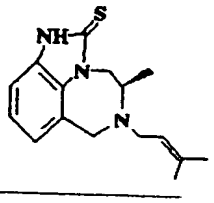

II

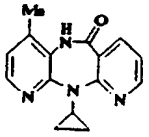

A new generation of non-nucleoside anti-HIV agents, such as TIBO [2] **I** and nevirapine [3] **II**, target reverse transcriptase (RT) of HIV-1. TIBO, nevirapine and their derivatives all seem to bind to the same site of RT [4]. It was recently established [5, 6] that TIBO and nevirapine bind to the same site of RT. Attempts are in progress to develop new and more active structures on the base of these two leads. However TIBO and nevirapine derivatives have a common serious drawback: resistant viral strains emerge after 2–3 weeks of clinical evaluation [7]. Low oral bioavailability (7–10%) established for TIBO [8, 9] also limits its applicability.

Significant attention has recently been paid to non-RT HIV inhibitors. For instance, the compound **III** (Ro 24-7429) was identified as an inhibitor of Tat, a protein which is a strong positive regulator of HIV replication [10]. Another example is non-peptidic protease inhibitor **VI** (XM-323) [11], discovered not

III

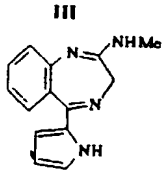

VI

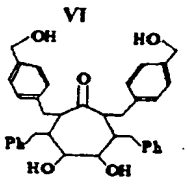

V

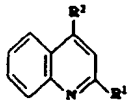

*Correspondence and reprints.
†On post-doctoral leave from the Institute of Physiogically Active Compounds, Russian Academy of Sciences, Chernogolovka, Russia.

Table I. Anti-HIV-1 activity (EC_{50}) in human PBM cells, cell toxicity (MTC), dipole moment (μ_1) of R^1 and shape descriptor ($(L/W)_2$) of R^2.

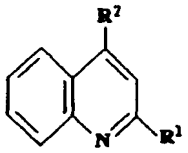

*Compound**	R_1	R_2	EC_{50} (μm)	$-log\ (EC_{50})$	MTC (μm)	μ_1	$(L/H)_2$
14	Ph	$NHCHMe_2$	100	−2.00	> 100	0.078	1.24
15	Ph	$NHCH_2CHMe_2$	50.6	−1.70	100	0.078	2.11
16	Ph	$NHCMe_3$	100	−2.00	100	0.078	1.10
17	Ph	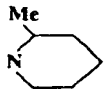	26.4	−1.42	100	0.078	1.83
18	Ph	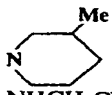	16.7	−1.22	100	0.078	1.83
19	Ph	$NHCH_2CH_2NMe_2$	10.0	−1.00	100	0.078	2.66
20	Ph	$N(Et)CH_2CH_2NMe_2$	34.3	−1.54	100	0.078	1.65
21	Ph	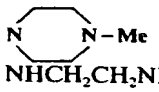	34.8	−1.54	100	0.078	2.40
22	4-FC_6H_4	$NHCH_2CH_2NMe_2$	13.2	−1.12	100	−0.107	2.66
23	4-ClC_6H_4	$NHCH_2CH_2NMe_2$	100.0	−2.00	100	−0.062	2.66
24	4-BrC_6H_4	$NHCH_2CH_2NMe_2$	44.2	−1.65	100	−0.013	2.66
25	4-$MeOC_6H_4$	$NHCH_2CH_2NMe_2$	10.4	−1.02	10	0.091	2.66
26	4-MeC_6H_4	$NHCH_2CH_2NMe_2$	4.47	−0.65	10	0.100	2.66
27	2-Pyridyl	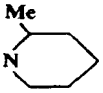	4.24	−0.63	100	0.136	2.40
28	2-Pyridyl	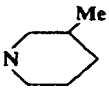	4.86	−0.69	100	0.136	2.40
29	2-Pyridyl	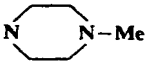	4.08	−0.61	100	0.136	2.40
30	2-Pyridyl	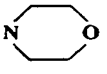	18.5	−1.27		0.136	1.45
31	2-Pyridyl	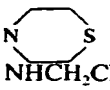	2.81	−0.45		0.136	1.48
32	2-Pyridyl	$NHCH_2CH_2NMe_2$	1.35	−0.13	100	0.136	2.66
33	2-Pyridyl	$N(Et)CH_2CH_2NMe_2$	13.2	−1.12		0.136	1.65

Table I. *(Continued.)*

*Compound**	R_1	R_2	EC_{50} (μm)	$-\log(EC_{50})$	MTC (μm)	μ_1	$(L/H)_2$
34	2-Pyridyl	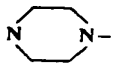	5.51	–0.74		0.136	2.40
35	3-Pyridyl		33.7	–1.53	100	0.141	1.57
36	3-Pyridyl		20.0	–1.30	100	0.141	1.83
37	3-Pyridyl	$NHCH_2CH_2NMe_2$	1.51	–0.18	> 100	0.141	2.66
38	3-Pyridyl	$N(Et)CH_2CH_2NMe_2$	24.2	–1.38	100	0.141	1.65
39	3-Pyridyl	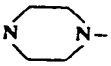	1.00	0.00	> 100	0.141	2.40
40	4-Pyridyl	$NHCH_2CH_2NMe_2$	36.9	–1.57	100	–0.033	2.66
41	4-Pyridyl	$N(Et)CH_2CH_2NMe_2$	100.0	–2.00	100	–0.033	1.65
42	4-Pyridyl	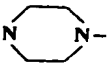	68.2	–1.83		–0.033	2.40
43	2-Furanyl	$NHCH_2CH_2NMe_2$	0.91	0.04	> 1	0.112	2.66
44	2-Furanyl	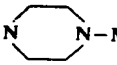	15.8	–1.20		0.112	2.40
45	2-Thienyl	$NHCH_2CH_2NMe_2$	0.57	0.24	10	0.127	2.66
46	2-Thienyl	$N(Et)CH_2CH_2NMe_2$	32.4	–1.51	100	0.127	1.65
47	2-Thienyl	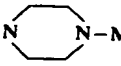	9.07	–0.96		0.127	2.40
53	Ph	NH_2	25.7	–1.41		0.078	1.50
54	2-Pyridyl	NH_2	8.56	–0.93	100	0.133	1.50
55	3-Pyridyl	NH_2	1.00	0.00	85.7	0.141	1.50
56	2-Thienyl	NH_2	34.3	–1.54	10	0.092	1.50

*In order to avoid any confusion we have kept the same method of numbering the compounds as was used in a previous report [11].

through random screening, as other anti-AIDS agents were, but through systematic computer-aided design.

Recently, a new class of non-nucleoside HIV-1 inhibitors has emerged **V** [12], represented by the 2-aryl-(or heteroaryl)-quinoline-4-amines **14–47, 53–56** (see table I). Some of these have demonstrated rather high *in vitro* activity against HIV-1, in combination with low toxicity.

Contrary to the majority of anti-HIV-1 series of compounds studied previously, **V** is quite suitable for classical or 3D QSAR (quantitative structure–activity relationships) as well as for molecular modeling. The series of 38 quinoline-4-amines possesses the following advantages making it appropriate for QSAR analysis: i) all the molecules in the set contain a relatively large common structural template which makes it possible to align the molecules for 3D analysis and to carry out a Hansch-type analysis; ii) the total interval of activity values is covered regularly by the compounds of the training set; and

iii) all structural changes are related to substituents attached to the two sites of common template with significant cross-variations which provide reliable analysis of substituent additivity.

The pharmacological action of these quinoline-4-amines was attributed [14] to the H-bond formation by the quinoline ring nitrogen (N1) with the hypothetical site probably situated on the viral RNA. Thus the variation of the electron density for the quinoline nitrogen should follow the variation of the inhibitory activity. However, this statement was contradicted by our preliminary study. We have carried out molecular modeling and quantum chemical calculations for compounds **14–47** and **53–60** and analysed the variation of electron density on N1. No correlation or trend between the N1 electron density and the ED_{50} or $\log(ED_{50})$ values was revealed. The following qualitative observations illustrate that: i) there is no difference in electron density on quinoline nitrogen atoms between compounds **33**, **34**, **38**, **39**, **41** and **42**, but activities in this small subseries vary from the highest to the lowest possible values; and ii) **39** is much more active than **40** despite the unfavorable difference in electron density of quinoline nitrogen in **39**. A Free–Wilson analysis of 21 compounds from this set [12] had modest statistic criteria ($r = 0.889$, $sd = 0.41$, $F = 5.67$) despite the significant number of adjustable parameters (NP = 9).

When atomic and substructural properties are not sufficient to reveal QSAR, an analysis of fields surrounding molecules can play the key role in understanding their pharmacological effect. We have already demonstrated the validity of the molecular electrostatic potential (MEP) to delineate the drug–receptor recognition process [13]. Another approach involving field processing is comparative molecular field analysis (CoMFA) [14]. CoMFA provides a consideration of total molecular field information in relation to chemical and biological molecular properties. CoMFA uses the PLS method [15] to reach an optimal reduction of molecular field data and to extract essential information from these data for modeling the activity. In the present study 3D QSAR were developed by CoMFA, providing the preliminary evaluation of anti-HIV-1 activity for newly designed molecules.

In addition to the field analysis, Hansch-type relationships may play a complementary role, providing an independent predicting model and making the whole study more reliable. This type of analysis uses multiple linear regression (MLR) to directly relate the activity to various properties of the substituents attached to the common template. In the present study, the results of molecular modeling and quantum chemical studies were used for selecting the substituent descriptors appropriate for Hansch-type models. In this study MLR were established, involving shape and electronic properties of the substituents.

To sum up, our study includes the following QSAR procedures: i) CoMFA; and ii) MLR with 3D and quantum chemical descriptors. The purpose of this study is to delineate a pharmacophore of 2-heteroaryl-quinoline-4-amine HIV-1 inhibitors in order to incorporate it into an efficient strategy of computer-aided drug design on anti-HIV-1 agents.

Methods

Molecular modeling

The whole set of quinoline-4-amines listed in table I were modeled using Sybyl 6.0 (Tripos Associates, Saint Louis, MO) on a Vax 3100. Low-energy conformations were determined with systematic search within Search option of Sybyl, using an unmodified Tripos force field [16]. The low energy conformations were then used as starting points in the optimization by the semiempirical quantum chemical AM1 method [17] (Interface/Mopac option of Sybyl). In addition, the rotational barriers were elucidated by the AM1 method, for the rotations around the bond between the quinoline and aryl, or heteroaryl rings. The barriers were found to be negligibly small, less than 1 kcal/mol, with minima at values between 25–35° for the dihedral angle between planes of quinoline and aryl rings.

QSAR

The training set consisting of 30 molecules, **14–21**, **23**, **24**, **27–30**, **32–42**, **44**, **46**, **47**, **53** and **54**, was selected for QSAR/MLR study. Compounds **25**, **26**, **31**, **43**, **45** and **56** were removed from our consideration as more toxic than the others. In fact, their high toxicity means that they have some additional mechanism in pharmacological action, which can interfere with their main action and therefore change its magnitude. Compounds **22** and **55** were dropped after preliminary QSAR studies as systematic outliers amid all the relationships we tried to construct. Such systematic outlying means that some latent external reasons make these compounds structurally incompatible with the others. The training set for CoMFA was selected according to the same rules as for MLR, with the only exception of compounds **53** and **54** which were additionally dropped from this set. The reason for dropping compounds **53** and **54** is a great difference in the steric environment of substituent R^2 for these compounds, compared with the others.

CoMFA options and alignment rules

The CoMFA method within Sybyl/QSAR was used for the 3D QSAR of the considered 28 quinoline-4-amines. The default probe of the sp^3 carbon atom with

a unity charge (+1) was used for field calculation in the grid points around the relevant molecules. The grid points were spaced by 2 Å in all three dimensions. Sybyl's fitting possibilities were used to align the compounds by superimposing the quinoline ring systems. The PLS runs with CoMFA column were made using the 'leave-one-out' validation technique, *ie* the number of cross-validation groups was the same as the number of molecules in the training set. This kind of cross-validation makes it possible to maximize the information capacity of the training set.

3D and quantum chemical descriptors

The shape descriptor (L/W) of the oblong character of substituent R^2 was calculated as ratio of the substituent's 3D length (L) to its width (W). Substituent R^2 was aligned along the *X*-axis of the Ruler option within the Sybyl/Graph option, keeping the quinoline ring in the plane of the screen, in order to reach the maximum value of the *X*-projection (see fig 1). The *X*-projection was then considered as the L parameter and *Y*-projection as the W parameter of the substituent R^2.

The projections of the dipole moment of the substituent R^1 on the *X*-axis (see fig 2) were calculated using the Sybyl/Mopac AM1 charges. All substituents were aligned by superposition of the planes of aryl rings and bonds between R^1 and quinoline ring. The

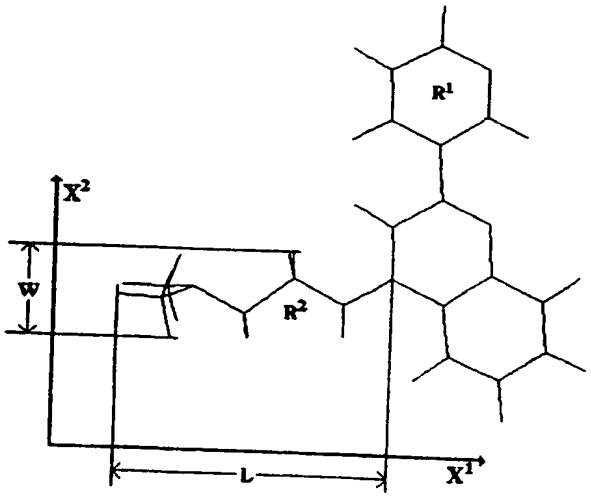

Fig 1. An alignment of the R^2 substituent for calculation of the L/W ratio on example of R^2 occurring in quinoline-4-amines **19**, **32**, **37** and **40**; the most possible measurement reached along x^1 axis is considered as length (L), the orthogonal measurement along x^2 is considered as width (W).

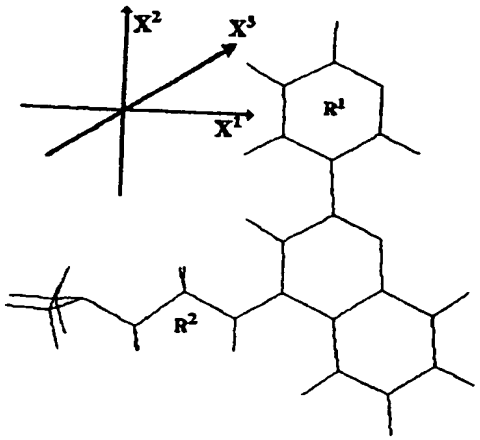

Fig 2. The directions of x^1, x^2 and x^3 axes used for derivation and calculation of the dipole projection (μ^1) in respect to the superimposed aryl or heteroaryl ring of R^1 substituent.

values of projections were calculated with the canonical formula: $\mu = \Sigma q_i r_i$, where q_i is the atomic charge and r_i is the projection of the charged site on the reference axis.

Results and discussion

QSAR studies by CoMFA

The cross-validated r^2 with the training set of 28 2-(aryl or heteroaryl)-quinoline-4-amines was 0.607 (with predictive *sd* of 0.391 and an optimum principal component number of 5). The conventional regression coefficient $r^2 = 0.920$ was calculated with the optimal number of principal components ($N_{pc} = 5$, $sd = 0.180$, $F(5,22) = 50.614$, $n = 28$). The new alignment obtained by fitting the molecules to the STDDEV* COEFF field within the Fieldfit option gave nearly the same model (cross-validated $r^2 = 0.612$, predictive *sd* = 0.375, optimum five principal components).

We must decide whether a cross-validated r^2 of 0.61 is good enough to proceed with further CoMFA capabilities. Otherwise the PLS model must be improved by trying different alignments, molecular models, *etc*. We used the information from the original study [12] in order to establish how good the model of the relevant activity data should be. The reported uncertainty in EC_{50} is expected to gradually increase from an estimated ±3 μM (0.47 in log scale) for the active molecules ($EC_{50} < 10$ μM) to ±10 (1.00 in log scale) for molecules with marginal activity. The standard error of predictions evaluated by CoMFA is 0.391. In fact this means that activity correlations between different

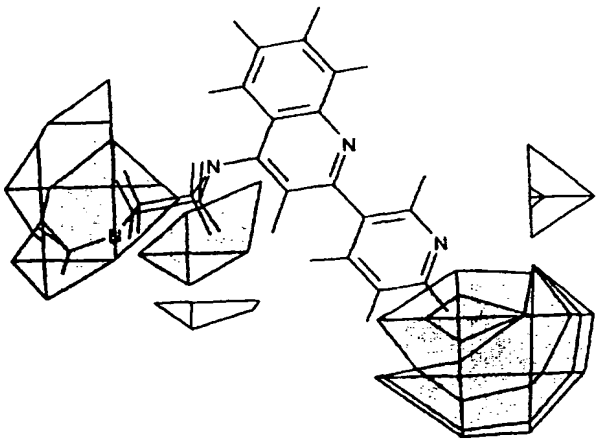

Fig 3. The CoMFA electrostatic field plot shows the regions in which structural variance causes the variance of anti-HIV-1 activity. Increasing positive electrostatic potential inside grey polyhedra or negative electrostatic potential inside white polyhedra should increase the activity.

series of measurements of the EC_{50} values may have an even worse correlation coefficient than that evaluated by CoMFA. On the other hand this means that there is no reason to search for better results, because the latter are most likely to be determined by chance effects.

The CoMFA plots obtained within the COMFA/Field/Graph options using the Contour and Contribution options with STDEV*COEFF field are shown in figures 3 and 4. The most active 2-(3-pyridyl)-quinolineamine **39** is shown in these figures to outline the sensitivity of the model. We can see that compound **39** already possesses most of the important structural features for increasing the activity as revealed by CoMFA. The regions in the plane of the molecule around R^1 are more important from the electrostatic point of view, as shown by presence of the differently shaded polyhedra. The region terminating R^2 encourages increases in the substituent's length. Nevertheless there is one structural feature which is not inherent to compound **39**: the large polyhedron and the small one behind the substituent R^2 show the usefulness of bulk and positive contributions in order to increase the activity. This feature is extracted from the moderately active compounds **17**, **18**, **27** and **28**. Thus, even by interpolation, we can improve the activity by attaching a methyl group to the *meta*-position of R^2 in 2-(3-pyridyl)-quinoline-4-amine **39**.

In general, CoMFA plots cannot be considered as a receptor model, because structural modulations do not usually concern active sites of molecules, *ie* the atoms which are actually contact with receptor. However in this study, CoMFA probably delineates some features of the receptor. For example, the region behind R^2 was marked as favorable for positively charged and bulky groups. However the alkyl groups in compounds **17**, **18**, **27** and **28**, which originated this structural hypothesis, do not affect the properties of the other molecular moieties. This means that these groups are probably important by themselves and fit in a hydrophobic pocket of the possible receptor.

QSAR studies using 3D and quantum chemical descriptors

The most important result of the LR study is the general equation:

$$-\log(EC_{50}) = 7.58(\pm 0.71)*\mu_1 + 0.70(\pm 0.09)*L/W_2 + 3.29(\pm 0.21) \quad [1]$$

$n = 30$, $R = 0.916$, $sd = 0.228$, $F(2,27) = 70.2$

This describes the whole set of 30 quinoline-4-amines, where μ_1 is the dipole moment related to the R^1 substituent and L/W_2 is the 3D oblong descriptor of R^2. Equation [1] is based upon approximately equal contributions of both R^1 and R^2 substituents. First, preliminary analyses were carried out in subseries with a fixed R^1 or R^2 substituent, in order to obtain this general relationship.

Two statistically sound subsets with a fixed substituent R^1 were selected. The first contained all the 2-phenylquinoline-4-amines (compounds **14–21**) and the second contained all the 2-(2-pyridyl)-quinoline-4-amines (compounds **27–30** and **32–34**). The qualitative analysis of these subsets shows that the shape of

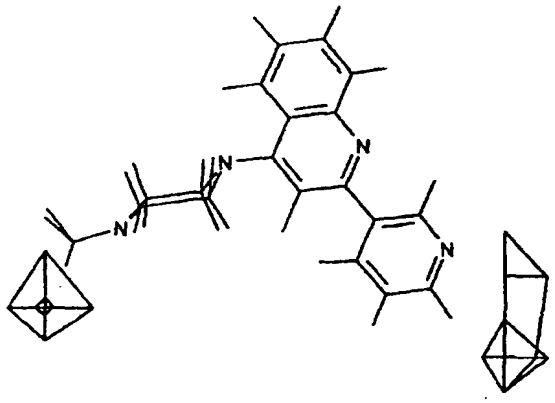

Fig 4. The ComFA steric field plot shows the regions in which structural variance causes the variance of anti-HIV-1 activity. Increasing bulk inside grey polyhedra and decreasing that inside white polyhedra should increase the activity.

substituent R^2 is an important factor leading to the activity changes. The series of correlations were tried with various geometric parameters of the substituent such as 2D and 3D length, width and volume. It was found that all these geometric parameters have similar activity trends, but each of them yields a significant number of outliers. Arithmetic combinations of the geometric parameters were also tried in various correlations in order to specify the shape contribution. The ratio of the two substituent dimensions, the L and W parameters, was derived. This ratio was established to be the best for the correlation between shape and activity within the subsets studied.

$$-\log(EC_{50}) = 0.56(\pm0.12)*L/W_2 + 4.05(\pm0.18) \quad [2]$$
$n = 8, R = 0.903, sd = 0.236, F(1,6) = 31.35$

$$-\log(EC_{50}) = 0.64(\pm0.14)*L/W_2 + 4.21(\pm0.19) \quad [3]$$
$n = 7, R = 0.89, sd = 0.231, F(1,5) = 29.71$

Although this descriptor was derived artificially, it has clear geometric sense. L/W expresses the oblong degree of the R^2 substituent.

Researching factors responsible for activity variance was carried out within subsets of compounds with fixed R^2 substituents. As the majority of R^1 substituents have the same shape, this particularly means that electrostatic contribution is essential for activity changes. Electrostatic models of increasing complexity were tried for substituent R^1 to describe its effect on activity. The simplest model is the effective point charge, expressed as the sum of charges on R^1 constituent atoms or a charge on one of the atoms of R^1. The effective point charge, nevertheless, was not found to be a good descriptor of R^1 substituent effect. The next level of complexity among electrostatic models is the dipole moment, expressing the polarity of a molecule or a fragment. The total molecular dipole moments are usually used as polarity descriptors of molecules. If all the molecules in the set are aligned in the same cartesian coordinates, then the molecular dipole moments will point to the different directions in the 3D space. The small molecules can easily orientate themselves in the space in order to point their dipoles toward the charged sites of a relevant receptor. However the orientation of the larger molecules and especially of their constituent fragments is not determined by their dipole moments only. In this case, a projection of the dipole moment onto an axis, pointing to the corresponding charged site of the receptor, is more important than the total dipole moment. The choice of the most important direction was made for the set of quinoline-4-amines in the plane of the aryl or heteroaryl ring of the R^1 substituent. First, the dipole components on axes X_1 and X_2 (see fig 2) were calculated. The choice of the X_1 and X_2 directions is arbitrary and does not affect the final result. The correlations of the activity with components calculated in both subsets were rather poor. The next hypothesis was to use the interdirection pointing to the nitrogen at position 3 of the aryl substituent. This direction was chosen because the 3-pyridyl R^2 has the best score as a contributor to activity, as was revealed by Free–Wilson analysis [12], and this could be observed qualitatively. The correlations of activity with this descriptor happened to have satisfactory criteria:

$$-\log(EC_{50}) = 0.81(\pm0.27)*\mu_1 + 2.1.(\pm0.11) \quad [4]$$
$n = 8, R = 0.891, sd = 0.331, F(1,6) = 34.28$

$$-\log(EC_{50}) = 0.95(\pm0.09)*\mu_1 + 1.82(\pm0.17) \quad [5]$$
$n = 7, R = 0.903, sd = 0.322, F(1,5) = 26.23$

Thus this descriptor was used in the final MLR (equation [1]), which, together with the geometric shape descriptor of R^2, has the best statistic criteria, which could be expected from the data studied.

Generalized 3D model of a quinolineamine lead

It is noteworthy to underline that CoMFA and MLR studies are in good agreement. This notable result can be expressed as follows: i) the axis onto which dipoles were projected to calculate the quantum chemical descriptors for the MLR points exactly toward the region marked by the CoMFA as favorable for increasing the negative electrostatic potential; and ii) the location of the region identified by CoMFA as favorable for bulky groups causes R^2 substituent to have a greater L/W ratio. This means that the two independent methods provide the same guidelines for a rational drug design.

The generalized 3D model of an active quinolineamine derived from the above results is presented in figure 5. The quinoline moiety emerges in all compounds, therefore it cannot be confirmed or eliminated by this study as a certainly necessary structure element. Thus, it is conditionally included in this model as a heteroaromatic system. A dipole carrier group is attached to the heteroaromatic system. The angle between the plane which contains the dipole and the heteroaromatic plane is around 30°. The angle between the bond connecting the dipole carrier group with the aromatic system and the direction of the dipole is around 120°. The lipophilic group is attached to the heteroaromatic system at 3–3.5 Å from the dipole carrier group. The length of this lipophilic moiety is not limited by the models obtained in this study. Single branching of the main lipophilic chain favors the activity, but double branching suppresses it. At least one amino group is needed, probably to produce a negative electrostatic field in the region between the lipophilic and dipole carrier groups.

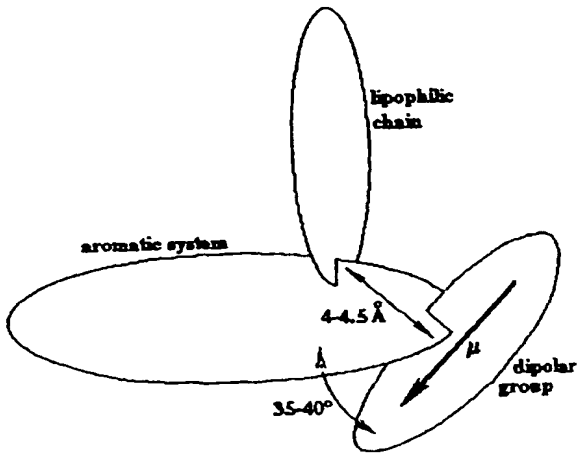

Fig 5. The generalized 3D model of a 2-heteroarylquinolin-4-amine lead. The aromatic system (quinoline moiety) is in the plane of the figure. The plane of polar substituent forms a dihedral angle of 35–40° with the plane of the aromatic system. The long lipophilic fragment is attached in 44.5 Å from the polar group.

One consequence that can be derived from the above 3D model should be underscored. The quinolineamines are not necessarily the best class of compounds that fit this model. Moreover, the ring of the aromatic substituent, forming the angle of around 30° with the quinoline aromatic ring, hides the quinoline nitrogen. Thus, it is hardly probable that this nitrogen represents the binding site with the biological receptor, as was previously proposed [12].

Conclusions

The 3D QSAR analyses by the CoMFA and MLR methods were carried out on the new series of 2-(aryl or heteroaryl)quinoline-4-amine HIV-1 inhibitors. Two new descriptors were derived from the 3D molecular structures for the MLR models. One of them represents the shape contribution of the amino-substituent and the other represents the projection of R^1 dipole moment on the direction pointing to a probable receptor site.

The generalized 3D model of a quinolineamine lead was derived using the results of the QSAR study. This generalized model suggests that other classes of compounds can have the same type of HIV-1 inhibitory action.

Both CoMFA and MLR studies indicate that the type of action is probably different from that proposed in the original study [1]. It is more probable that substituents R^1 and R^2 interact with the biological receptor rather than the N1 nitrogen.

Work is underway to perform classical biochemical assays. The knowledge of the biological target of compounds studied will allow us to carry out more orientated design of novel molecules. However, the methods used in this work do not depend on the biological mechanism. New molecules were designed using QSAR obtained by us. The experimental results obtained in biological assays for studied and novel molecules will be reported in forthcoming communications.

Acknowledgments

The authors wish to thank the Ministère de l'enseignement supérieur et de la recherche for a grant to KDB. We also thank A Astruc for linguistic assistance in preparing this manuscript. We thank Tripos, France (Palaiseau) for facilities in using Sybyl 6.0.

References

1 Mitsuya H, Broder S (1987) *Nature (Lond)* 325, 773–778
2 Kukla MJ, Breslin HJ, Powels R *et al* (1991) *J Med Chem* 31, 746–751
3 Hargrave KD, Proudfoot JR, Grozinger KG *et al* (1991) *J Med Chem* 3, 2231–2241
4 Kohstaedt LA, Wang J, Friedman JM, Rice PA, Steitz TA (1992) *Science* 256, 1783–1790
5 Scoog MT, Hargrave KD, Miglietta JJ, Kopp EB, Merluzzi VJ (1992) *Med Res Rev* 12, 27
6 Cohen CA, Hopkins J, Ingraham RH *et al* (1991) *J Biol Chem* 266, 14670–14674
7 De Clercq E (1994) *Biochem Pharmacol* 47, 155–169
8 De Vit S, Hermans P, Sommereijns B *et al* (1992) *Antimicrob Agents Chemother* 36, 2661
9 Hattox S (1992) VIII Int Conf AIDS/III STD World Congress, Abstr 3591
10 Lan PYS, Jadhav PK, Eyermann CJ *et al* (1994) *Science* 263 380–384
11 Strekowski L, Mokrosz MJ, Honkan VA *et al* (1991) *J Med Chem* 34, 1739–1746
12 Strekowski L, Mokrosz MJ, Harden DB, Mokrosz JL, Wilson WD (1990) *In: Adv Chemother AIDS* (Diasio RB, Sommdossi JP, eds) Pergamon, NY, USA
13 Boudon A, Szymoniak J, Chretien JR (1988) *Eur J Med Chem* 23, 365–371
14 Cramer RDIII, Patterson DE, Bunce JD (1988) *J Am Chem Soc* 110, 5959–5967
15 Wold S, Albano C, Dunn WJ *et al* (1984) *In: Chemometrics: Mathematics and Statistics in Chemistry* (B Kowalski, ed), Reidel, Dordrecht, The Netherlands
16 Clarc M, Cramer RDIII (1989) *J Comput Chem* 10, 92–1012
17 Dewar MJS, Zoebich EG, Healy EF, Stewart JJP (1985) *J Am Chem Soc* 107, 3902–3909

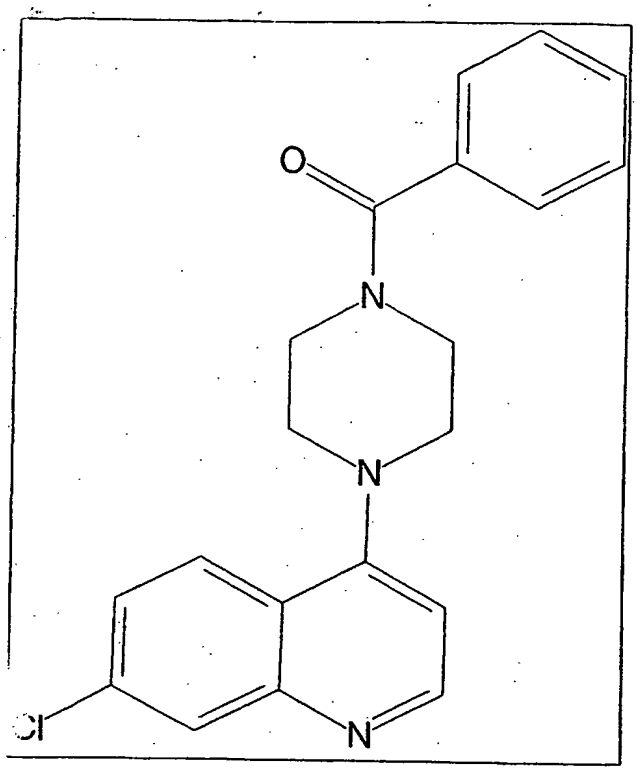

XP-002255284

P.D. 00:00:00
P. 1-3
3

Substance

Beilstein Registry Number	**7386604**
Chemical Name	[4-(7-chloro-quinolin-4-yl)-piperazin-1-yl]-phenyl-methanone
Autoname	[4-(7-chloro-quinolin-4-yl)-piperazin-1-yl]-phenyl-methanone
Molecular Formula	$C_{20}H_{18}ClN_3O$
Molecular Weight	351.83
Lawson Number	28000, 27421, 10581
Compound Type	heterocyclic
Constitution ID	6280178
Tautomer ID	6925684
Beilstein Reference	6-23
Entry Date	1996/04/26
Update Date	1997/02/03

Reaction

Reaction ID	*4379692*
Reactant BRN	*125359* 4,7-dichloro-quinoline *8060* 1-benzoyl-piperazine
Product BRN	**7386604** [4-(7-chloro-quinolin-4-yl)-piperazin-1-yl]-phenyl-methanone
No. of Reaction Details	1
Reaction Classification	Preparation
Yield	67 percent (BRN=7386604)
Reagent	K2CO3
Solvent	dimethylformamide
Time	8 hour(s)
Other Conditions	Heating

Ref. 1	*5999135*; Journal; Tripathi, R. C.; Saxena, M.; Chandra, S.; Saxena, Anil K.; IJSBDB; Indian J.Chem.Sect.B; EN; 34; 2; 1995; 164-166;

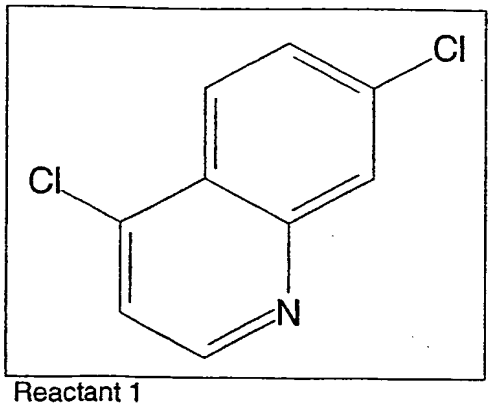

Reactant 1

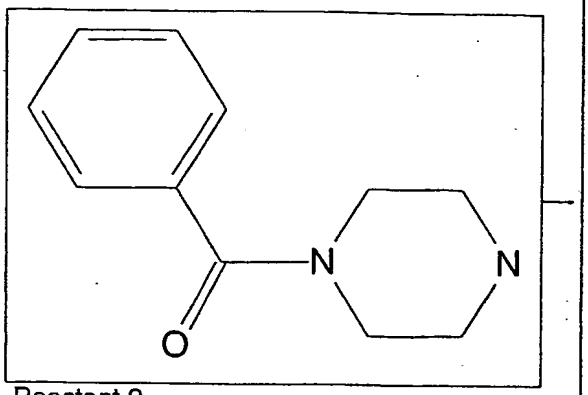

Reactant 2

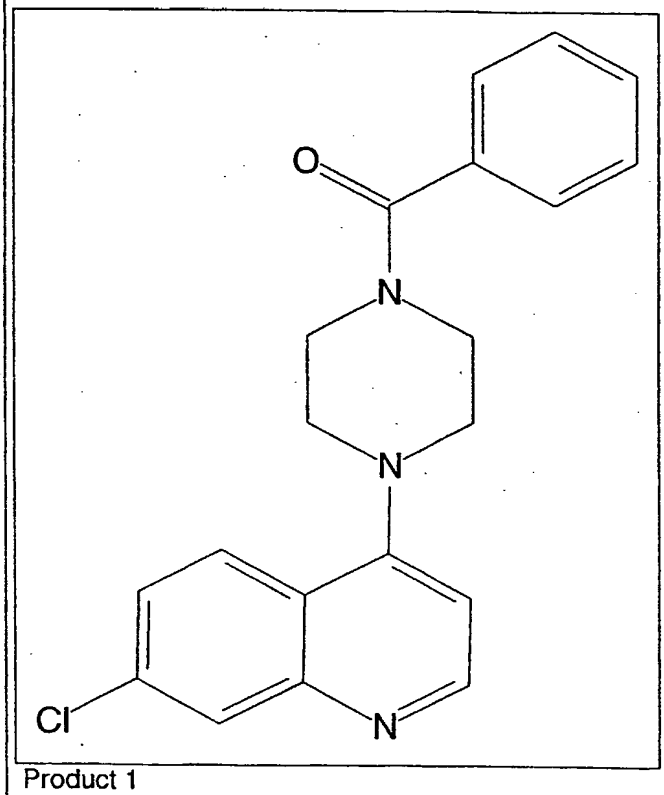

Product 1

Melting Point

VALUE (MP) C	Solvent (.SOL)	Note	Ref.
158			1

Ref. 1	*5999135*; Journal; Tripathi, R. C.; Saxena, M.; Chandra, S.; Saxena, Anil K.; IJSBDB; Indian J.Chem.Sect.B; EN; 34; 2; 1995; 164-166;

Pharmacological Data

Note 1	activity on reversal of chloroquin resistance: inactive at a dose of 3 mg/kg
Ref. 1	*5999135*; Journal; Tripathi, R. C.; Saxena, M.; Chandra, S.; Saxena, Anil K.; IJSBDB; Indian J.Chem.Sect.B; EN; 34; 2; 1995; 164-166;